Spatial localization of moment deficits in southern California

Brendan J. Meade[1] and Bradford H. Hager

Department of Earth, Atmospheric and Planetary Sciences, Massachusetts Institute of Technology, Cambridge, Massachusetts, USA

Received 20 July 2004; revised 12 January 2005; accepted 31 January 2005; published 14 April 2005.

[1] The balance between interseismic elastic strain accumulation and coseismic release defines the extent to which a fault system exhibits a surplus or deficit of large earthquakes. We calculate the regional moment accumulation rate in southern California based on a fault slip rate catalog estimated from a block model of interseismic deformation constrained by GPS measurements. The scalar moment accumulation rate, $17.8 \pm 1.1 \times 10^{18}$ N m/yr, is approximately 50% larger than the average moment release rate over the last 200 years. Differences between the accumulated and released elastic displacement fields are consistent with moment deficits that are localized in three regions: the southern San Andreas and San Jacinto faults, offshore faults and the Los Angeles and Ventura basins, and the Eastern California Shear Zone. The moment budget could be balanced by coseismic events with a composite magnitude of $M_w \approx 8$.

Citation: Meade, B. J., and B. H. Hager (2005), Spatial localization of moment deficits in southern California, *J. Geophys. Res.*, *110*, B04402, doi:10.1029/2004JB003331.

1. Introduction

[2] The potential for large earthquakes is typically characterized by one of three approaches. The first is the calculation of moment magnitudes consistent with the size of potential fault rupture areas [e.g., *Dolan et al.*, 1995; *Shaw and Shearer*, 1999; *Meade et al.*, 2002]. A second method is to evaluate the completeness of historical earthquake catalogs using Gutenberg-Richter style magnitude-frequency statistics [e.g., *Working Group on California Earthquake Probabilities*, 1995 (hereinafter referred to as WGCEP95); *Stein and Hanks*, 1998 (hereinafter referred to as SH98)]. The third approach is to assess the balance between interseismic moment accumulation and coseismic moment release rates [e.g., WGCEP95; SH98; *Ward*, 1998a]. Moment is a measure of the size of an earthquake that depends on the area of the rupture surface, the average fault slip, and the rigidity or shear modulus. The potency, or geometric moment, of an earthquake is the product of the average slip over the rupture area, $P = \bar{s}A$ [e.g., *Ben-Zion*, 2001]. Geodetic studies of earthquake slip distributions typically assume an elastic Poisson body and therefore directly estimate potency, which is converted to moment by multiplying by the shear modulus, μ. For the sake of continuity with the literature, we use moment throughout the rest of this paper and assume that the shear modulus is constant and equal to 3×10^{10} Pa.

[3] The total coseismic moment release, M_0^R, is defined as the sum of scalar moments in an earthquake catalog of duration T, and the mean moment release rate is $\dot{M}_0^R = M_0^R/T$. We define the total moment accumulation rate as the sum of moment accumulation rates from each fault segment, $\dot{M}_0^A = \mu \dot{s} A$, ($\dot{s}$ slip rate). Multiplying $\dot{M}_0^A$ by T gives the total moment accumulation M_0^A assuming that slip rates have been constant through time. *Kostrov* [1974] defined moment accumulation rate as $\dot{M}_0^A = 2\mu\alpha H\dot{\varepsilon}$, where H is the seismogenic thickness, $\dot{\varepsilon}$ is the uniform regional strain rate, and α is the area, not of the fault surfaces but of the deforming region (e.g., southern California). This method provides a lower bound on moment accumulation rate in the sense that regional strain rate data do not include information relating surface strain rates to the fault system geometry, where moment is released during earthquakes. In contrast, moment accumulation rates calculated from geodetically constrained slip rate models [e.g., *Meade and Hager*, 2005] (hereinafter referred to as MH05), account for the effects of localized interseismic strain accumulation near fault zones. Further, the surface strain rate method is potentially misleading because of the strain rate paradox, where strain rates are negatively correlated with fault locking depths ($\dot{\varepsilon}_{max} \sim D^{-1}$) and positively correlated with moment accumulation rates ($M_0^A \sim D$). Thus faults with fast slip rates and shallow locking depths are characterized by a relatively high strain rate yet a relatively low moment accumulation rate. The creeping segment of the San Andreas fault (SAF) north of Parkfield is the type locale.

[4] Regardless of the method employed, the question is the same: Has the rate of coseismic moment release, $\dot{M}_0^R$, kept up with the rate of moment accumulation, $\dot{M}_0^A$, over the duration of the earthquake catalog, T? A moment release rate greater than the accumulation rate, $\dot{M}_0^R > \dot{M}_0^A$, defines a moment surplus, and the converse, $\dot{M}_0^R < \dot{M}_0^A$, defines a deficit. The balance between moment accumulation and release rates can be expected to hold if five conditions are

[1]Now at Department of Earth and Planetary Sciences, Harvard University, Cambridge, Massachusetts, USA.

0148-0227/05/2004JB003331$09.00

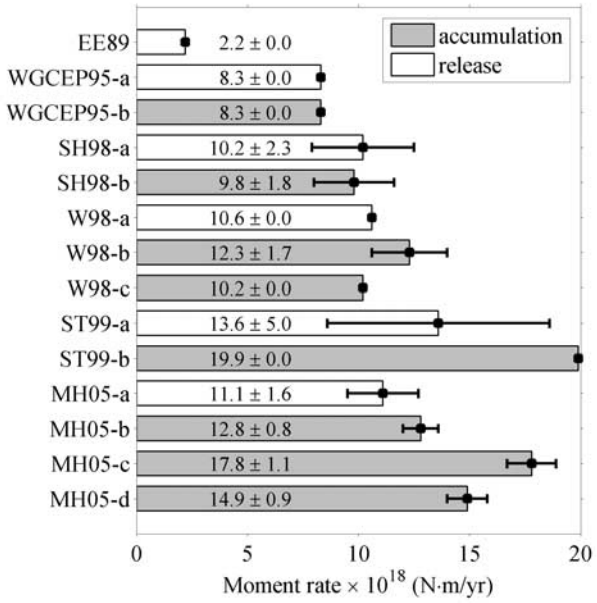

Figure 1. Moment accumulation and release rates in southern California. EE89, *Ekstrom and England* [1989] release rate; WGCEP95-a, WGCEP95 release rate; WGCEP95-b, WGCEP95 accumulation rate; SH98-a, SH98 release rate; SH98-a, SH98 accumulation rate; W98-a, *Ward* [1998a] release rate; W98-b, *Ward* [1998a] geologic accumulation rate; W98-c, *Ward* [1998a] geodetic accumulation rate; ST99-a, *Shen-Tu et al.* [1999] release rate; ST99-b, *Shen-Tu et al.* [1999] accumulation rate; MH05, this paper, release rate; MH05-b, this paper, geologic accumulation rate; MH05-c, this paper, preferred block model accumulation rate; and MH05-d, this paper, 11 km block model accumulation rate. The block model with a uniform 11 km locking depth decreases the goodness of fit to geodetic data by 30% compared with MH05's preferred model.

met. First, the effects of distributed dissipative processes, such as fracturing and folding, are negligible. Second, creep events are either absent or accounted for. Third, the largest sized event in the earthquake catalog is representative of the largest sized event that occurs in the fault system. Large earthquakes dominate the moment budget [e.g., MH05], therefore moment release rate may be severely underestimated if the earthquake catalog lacks the maximum size event. Fourth, the moment accumulation rate (i.e., fault slip rates) must be constant over the length of the earthquake catalog. The fifth condition is that the earthquake catalog must be long enough to reflect characteristic fault system activity. In southern California, the length of the historical earthquake catalog (200 years) is comparable to the average recurrence interval for large earthquakes on the SAF [e.g., *Sieh et al.*, 1989]. Most other faults in the southern California fault system have much longer recurrence intervals [e.g., *Rubin et al.*, 1998; *Rockwell et al.*, 2000]. Thus the earthquake catalog is too brief to encompass an entire earthquake cycle across all fault zones. However, if the catalog sees the average behavior of many long recurrence interval faults, then it may be sufficient to assess the balance between moment accumulation and release rates [*Ward*, 1998a].

[5] Complex temporal behavior, such as the clustering of earthquakes, may increase the time interval over which moment accumulation and release will balance from hundreds to thousands of years [e.g., *Rockwell et al.*, 2000]. The brevity of the historical earthquake catalog precludes the calculation of moment balance since the last known rupture of each fault segment or the average over a clustered earthquake cycle. However, we can assess whether or not moment accumulation and release rates balance over the last two centuries. This calculation can be thought of as the deviation from some reference quasiperiodic earthquake cycle.

2. Regional Moment Balance

[6] Regional moment balance in southern California has been studied extensively over the last fifteen years (Figure 1). *Ekstrom and England* [1989] demonstrated that a 10-year-long earthquake catalog was too brief to assess the balance between moment accumulation and release rates. WGCEP95 reported a moment release rate of 8.3×10^{18} N m/yr on the basis of an earthquake catalog that included a $M_w = 7.8$ Fort Tejon event (1857), but without the $M_w = 7.6$ Owens Valley earthquake (1872). *Field et al.* [1999] noted that the moment magnitude relationship used by WGCEP95 under predicts moment by 12–25% compared with the widely used *Hanks and Kanamori* [1979] relationships. SH98 calculated a $10.2 \pm 2.3 \times 10^{18}$ N m/yr moment release rate using an expanded earthquake catalog, and argued that there was no moment deficit in southern California on the basis of both plate motion and geologic slip rate moment accumulation models. *Ward* [1998a] calculated accumulation and release rates similar to SH98. Using the *Kagan* [2004] (hereinafter referred to as K04) earthquake catalog, we estimate an average moment release rate of $11.1 \pm 1.6 \times 10^{18}$ N m/yr over the last 200 years.

[7] Moment accumulation rates can be calculated from regional-scale fault slip rate models. *Petersen et al.* [1996] (hereinafter referred to as P96) compiled an extensive list of geologically determined fault slip rates in southern California. MH05 used a block model to invert GPS measurements of interseismic deformation for plate motions and kinematically consistent fault slip rates. The block model includes the effects of block rotation and interseismic strain accumulation consistent with a simple earthquake cycle model. MH05 argued that geodetic observations of interseismic deformation do not provide significant evidence for long-term viscoelastic deformation in southern California and that the block model slip rate estimates are not significantly influenced by postseismic deformation. Specifically, the large strain gradients observed near faults that are thought to be late in their earthquake cycles (e.g., southern San Andreas) are inconsistent with the postseismic relaxation of a relatively weak lower crust/upper mantle with a viscoelastic Maxwell rheology. The geologic and geodetic slip rate models average fault behavior over significantly different timescales (10^5–10^6 years versus 15 years) and may reflect different aspects of time-dependent fault system behavior. We focus on the implications of the MH05 model because it is consistent with plate motion constraints, fault

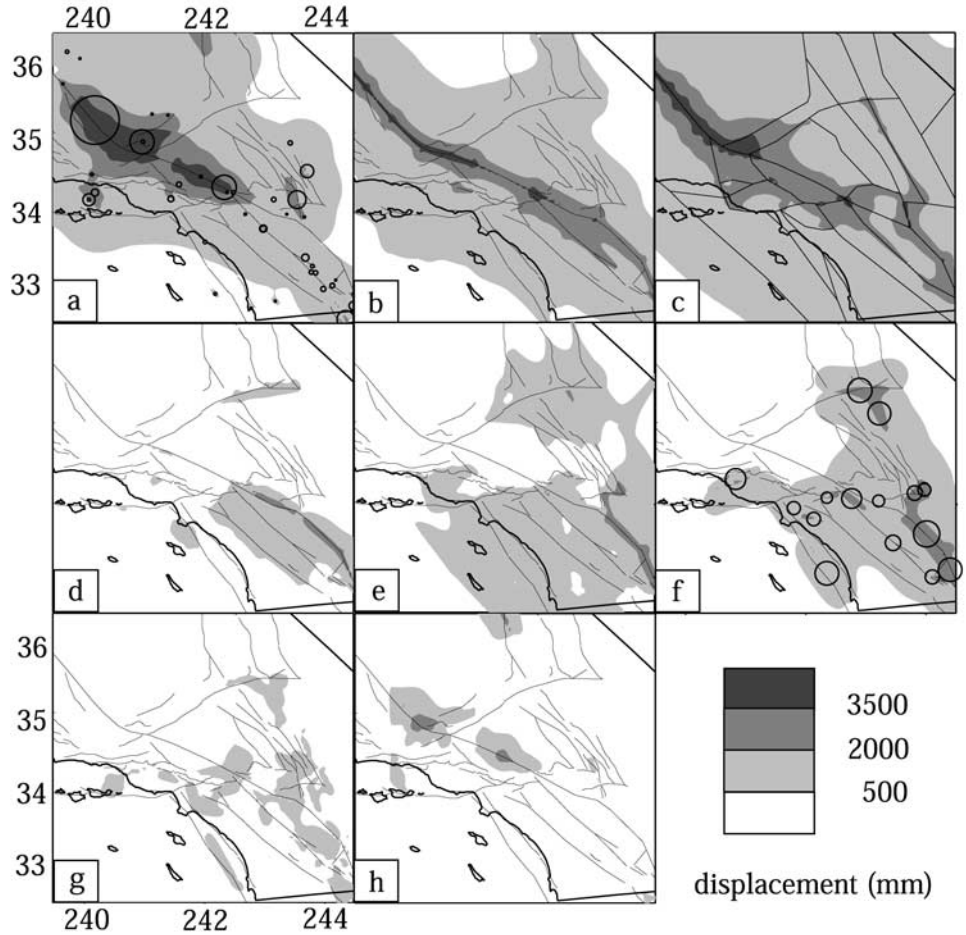

Figure 2. Elastic displacement fields in southern California. The fields shown are (a) released earthquake displacements, D_R^{K04}, with historical earthquake epicenters and magnitudes, (b) accumulated geologic displacements D_A^{P96}, (c) accumulated block model interseismic displacements, D_A^{MH05}, (d) differential geology-earthquake displacements, ΔD_{K04}^{P96}, (e) block model deformation deficit field, ΔD_{K04}^{MH05}, (f) model deficit source displacements with potential source locations and magnitudes, (g) residual displacement field, and (h) block model deformation surplus field. Displacements are shaded by magnitude with contours drawn at 500, 2000, and 3500 mm intervals. The thin black lines in Figures 2a, 2b, 2d, 2e, 2f, 2g, and 2h are geologic fault traces, while the thin black lines in Figure 2c are the block model boundaries from MH05.

system geometry, a simple model of the earthquake cycle, and GPS observations of interseismic deformation that overlap with nearly 10% of the span covered by the historical earthquake catalog. In contrast, the earthquake catalog overlaps, at most 1%, with of the period of time over which geologic slip rates have been averaged. In all calculations, southern California is defined as the region within 32.5–36.5° latitude and 239.5°–244.5° longitude (Figure 2).

[8] Geologically determined slip rates provide information about long-term moment release rates, while slip rates inferred from models of interseismic geodetic observations directly constrain present-day moment accumulation rates. Assuming that slip rate estimates are applicable to, and have been constant throughout, the last 200 years the geologic [P96] and geodetically constrained block model [MH05] slip rate catalogs are consistent with a moment accumulation rates of $12.8 \pm 3.7 \times 10^{18}$ N m/yr and $17.8 \pm 1.1 \times 10^{18}$ N m/yr, respectively. The block model moment accumulation rate uncertainty is calculated by propagating the uncertainty in the relative motion between the Pacific and North American plates and reflects the fact that the block model slip rates covary because of path integral constraints that insure internally consistent fault slip rate estimates. Thus, on a percentage basis, the moment accumulation rate uncertainty is greater for any given fault than it is at the regional scale. The MH05 derived moment accumulation rate is 50% larger than previous estimates [WGCEP95; SH98; *Ward*, 1998a]. *Shen-Tu et al.* [1999] calculated a comparable 19.9×10^{18} N m/yr moment accumulation rate using a strain rate approach that may be subject to the strain rate paradox. We find relatively high moment accumulation rates for three reasons. First, the population of faults in MH05 is relatively large, with approximately 50,000 km^2 of fault system surface area. Second, the MH05 model allows a fault to have two

components of slip (e.g., strike and dip slip). Third, in the MH05 model, the geodetic data are projected onto the fault system geometry by using a block model that includes the effects of interseismic strain accumulation. This means that the MH05 block model includes the details of how deformation is partitioned across the fault system rather than assuming uniform simple shear.

[9] The simplest interpretation of imbalance between moment accumulation and release rates is that there is a substantial deficit of large earthquakes in southern California over the last two centuries. However, the interpretation of regional moment balance calculations is challenging because of uncertainties in the size of the largest earthquake, the extent of the study region, and a lack of information about the location of moment deficits.

3. Spatial Localization of Moment Deficits

[10] Both the historical earthquake catalog and fault slip rate models contain spatial information (epicenters and fault system geometry) that can be used to localize regions where moment deficits are largest. Elastic displacement fields [*Okada*, 1985] allow us to compare the focal mechanism and slip rate catalogs with a mechanical model for strain accumulation and release. This method also allows for a degree of spatial smoothing, which has the advantage of not requiring the precise alignment of epicenters and faults, but the disadvantage of making it difficult to separate the contributions from nearby structures. To calculate the released displacement field, D_R, we use *Wells and Coppersmith*'s [1994] empirical scaling relations to estimate the slip and an approximate rupture geometry for the 65 $M_w \geq 6$ earthquakes that have occurred since 1800 [K04]. The lone exception is the 1857 Fort Tejon event ($M_w = 7.9$), for which we use the geometry and slip distribution described by *Sieh* [1978]. The largest elastic displacements are focused near the epicenters of the 1812, 1857, and 1952 events near the Mojave and Carrizo segments of the SAF (Figure 2a). The northern Eastern California Shear Zone (ECSZ) also has peak displacements of more than 4 m due to the 1872 Owens Valley earthquake. In contrast, the magnitude of elastic displacement is approximately 25% smaller along the San Jacinto fault (SJF), southern SAF, Los Angeles basin, offshore faults, and the central ECSZ (Figure 2a).

[11] The total elastic displacement field accumulated over the interseismic period, D_A, is calculated similarly to D_R, except that the sum is over all fault segments, and slip is replaced by the slip rate multiplied by the duration of the earthquake catalog, $s = \dot{s}T$. Both D_A^{P96} (Figure 2b) and D_A^{MH05} (Figure 2c) show large displacements along the entire length of the SAF and SJF. However, D_A^{MH05} also shows large amounts of deformation in the ECSZ and along the offshore faults while D_A^{P96} does not. The difference between the accumulated and released displacement fields, $\Delta D_R^A = D_A - D_R$, allows us to identify areas where moment accumulation and release balance over the past two centuries and those where they do not. Displacement surpluses and deficits correspond to $\Delta D_R^A < 0$ and $\Delta D_R^A > 0$ respectively. The most striking feature of both the $\Delta D_{\mathrm{K04}}^{\mathrm{P96}}$, and $\Delta D_{\mathrm{K04}}^{\mathrm{MH05}}$ displacement fields is the deformation deficit along the SJF and southern SAF (Figures 2d and 2e). The displacement deficit calculated from geologic slip rates, $\Delta D_{\mathrm{K04}}^{\mathrm{P96}}$, implies a larger moment deficit along the San Bernardino segment of the SAF (SBSAF) than do geodetic rates, $\Delta D_{\mathrm{K04}}^{\mathrm{MH05}}$, because of the fact that the geologically estimated slip rate [*Weldon and Sieh*, 1985] is 5 times larger than that estimated from geodesy [MH05]. The $\Delta D_{\mathrm{K04}}^{\mathrm{MH05}}$ deficit map shows significant displacement deficits in three regions: (1) the SJF and southern SAF, (2) the offshore faults and Los Angeles and Ventura basins, and (3) the ECSZ. While $\Delta D_{\mathrm{K04}}^{\mathrm{P96}}$ shares the southern SAF deficit, it has less significant deficits in the LA basin and ECSZ due to the fact that the P96 catalog has less localized slip in these two regions.

[12] The displacement deficits (Figures 2d and 2e) can be used to estimate the magnitudes and locations of earthquake sources that could potentially balance the moment budget. For each of the three major deficit regions we use a directed forward search algorithm to refine loosely constrained source parameters for model coseismic events that minimize the residual between the model and $\Delta D_{\mathrm{K04}}^{\mathrm{MH05}}$ displacement fields (Figures 2f and 2g). Using 15 potential earthquake sources, we find a composite moment deficit that is consistent with our regional deficit estimate and approximately equivalent to a $M_w \approx 8$ event.

[13] The eight sources along the SJF and southern SAF yield a total moment deficit equivalent to a $M_w = 7.8$ event (Figure 2f) with the Indio segment having the largest individual magnitude ($M_w = 7.4$). Along the Indio segment of the SAF, strain may have been accumulating for longer than we have assumed, as the last known rupture on this segment was ~330 years ago [*Sieh et al.*, 1989]. The San Bernardino segment of the SAF has the smallest deficit due to the relatively slow ~5 mm/yr geodetically constrained slip rate [MH05]. No source is associated with the Imperial fault due the fact that it is allowed to creep in the MH05 model.

[14] In the greater Los Angeles region (including the Ventura basin and offshore faults) the combined magnitude of 5 model sources is $M_w = 7.7$, with the largest model earthquake ($M_w = 7.4$) located west of the Northridge rupture along the southern edge of the Ventura basin. Two $M_w = 7.0$ sources, related to either the Puente Hills or Elysian Park thrust faults, are situated beneath metropolitan Los Angeles. While both of these faults are blind, *Dolan et al.* [2003] suggested that the structure of near-surface folds is consistent with growth during $M_w \geq 7.2$ earthquakes. *Rubin et al.* [1998] also found evidence for large slip events on the Sierra Madre fault and estimated the interevent times for the last two large ruptures as ~5000 years. Thus the earthquakes along the San Gabriel range front, and in the Los Angeles basin, may be infrequent but very large. To account for the entire offshore displacement deficit would require additional sources along structures such as the San Clemente fault. While the magnitude of the single potential offshore source is consistent with the total magnitude of the offshore deformation deficit, it is best considered a simple parameterization of deformation that is accommodated by a series of offshore faults [e.g., *Grant and Rockwell*, 2002].

[15] The moment deficit in the ECSZ may be the least well constrained because of the fact that rupture history prior to 1900 may be poorly documented [SH98]. On the other hand, both coseismic activity (1992 Landers, 1999

Hector Mine earthquakes) and geodetic measurements of interseismic deformation rates [*Sauber et al.*, 1994; *Savage et al.*, 1990; *Peltzer et al.*, 2001; MH05] suggest that the ECSZ is active today, and accommodates at least 12 mm/yr of motion between the western Mojave/Sierra block and the North American plate. The cumulative magnitude of the two model sources in the ECSZ is M_w = 7.5. One is aligned along the north-south trending Goldstone fault to the north of the Landers and Hector Mine ruptures. The other source is east-west trending along the Garlock, which acts as a single source parameterization to account for the deformation deficit that is due to the complex behavior associated with the numerous fault intersections in the ECSZ. While the MH05 model has less than 2 mm/yr of left-lateral slip on the eastern Garlock, the intersections with right-lateral faults (e.g., Blackwater, Airport Lake, Death Valley) give rise to fault normal deformation in addition to strike-slip motion.

[16] Moment accumulation rates are linearly dependent on fault locking depths. MH05's preferred model uses a 10-km locking depth for the SJF and ECSZ, and 15-km locking depth for the southern SAF and the faults in the greater Los Angeles region. Experiments with a range of locking depths on the southern SAF and SJF show that the goodness-of-fit criterion decreases by 118% and 18%, respectively, for 0- and 5-km locking depths, respectively, compared with the preferred model. In addition, the depth of maximum seismicity ranges from 10 to 20 km in this region [*Hauksson*, 2000], consistent with the locking depths in the MH05 model. The deepest locking depths in the MH05 model (22 km) are along the Carrizo segment of the SAF, where we find the largest moment surplus (Figure 2h). Therefore it seems unlikely that unphysical locking depth are responsible for the estimated moment deficits in southern California.

4. Discussion

[17] It may be the case that creep events/silent earthquakes relieve accumulated strain. Large, $M_W \approx 7$, events have been documented in subduction zones using continuous GPS data [e.g., *McGuire and Segall*, 2003]. Comparably sized events have not been discovered in the continental lithosphere in southern California or elsewhere. However, small magnitude events have been recognized. *Linde et al.* [1996] observed a M_w = 4.8 event with strain meter data along the SAF south of San Francisco and *Vincent et al.* [1998] and *Vincent* [2000] documented a M_w = 5.3–5.6 creep event on the southern most segment of the SJF (Superstition Hills segment). *Sieh and Williams* [1990] reported evidence for small magnitude near-surface creep along the Indio segment of the southern SAF. If aseismic slip events account for the observed moment deficits in southern California, then they should be observable using high-precision geodetic measurements. Assuming that the frequency of hypothetical creep events/silent earthquakes is consistent with the Gutenberg-Richter distribution and that ~50% of the moment release is silent, we would expect to observe $M_w \geq 6$ earthquakes, at a rate of ~0.16 events per year. Thus we expect at least one event with meter-scale near-field displacements to have occurred during the last 10 years. However, if the southern California fault system tends to have large ($M_w > 7$) characteristic earthquakes [e.g., *Sieh*, 1996], whether silent or not, there is a lesser probability that these events have occurred during the instrumented period. Further, the bulk of the upper crust is thought to be conditionally stable (velocity strengthening) in terms of the temperature-dependent rate-state friction models [e.g., *Scholz*, 1998] unlike the conditions inferred for silent earthquakes in subduction zones [e.g., *Dragert et al.*, 2001; *McGuire and Segall*, 2003]. Thus, unless 50% of the accumulated moment is released silently, the most physically consistent mechanism for alleviating moment deficits in southern California is a series of $M_w > 7$ coseismic events.

5. Conclusions

[18] Using a fault slip rate model constrained by GPS measurements of interseismic deformation we have found that there is a coseismic moment release deficit in southern California. The preferred moment accumulation rate, $17.8 \pm 1.1 \times 10^{18}$ N m/yr, is approximately 50% greater than the average moment release rate, $11.1 \pm 1.6 \times 10^{18}$ N m/yr, over the past two centuries. The southern San Andreas and San Jacinto faults, the greater Los Angeles region, and the Eastern California Shear Zone, exhibit elastic displacement deficits equivalent to moment magnitude 7.8, 7.7, and 7.5 events, respectively. Creep events and silent earthquakes could balance the moment budget without the need for coseismic deformation. The search for these phenomena will require additional geodetic data with greater spatial and temporal density than is currently available. Thus, while the seismicity rate deficit may have vanished [SH98; *Ward*, 1998b], new fault slip rate models [e.g., MH05] have made the moment deficit appear more clearly.

[19] **Acknowledgments.** This research was supported by the Southern California Earthquake Center. SCEC is funded by NSF Cooperative Agreement EAR-0106924 and USGS Cooperative Agreement 02HQAG0008. We thank Tom Hanks and Ross Stein for thoughtful reviews. This is SCEC contribution 824.

References

Ben-Zion, Y. (2001), On quantification of the earthquake source, *Seismol. Res. Lett.*, *72*, 151–152.

Dolan, J. F., K. Sieh, T. K. Rockwell, R. S. Yeats, J. Shaw, J. Suppe, G. J. Huftile, and E. M. Gath (1995), Prospects for larger or more frequent earthquakes in the Los Angeles metropolitan region, *Science*, *267*, 199–205.

Dolan, J. F., S. A. Christofferson, and J. H. Shaw (2003), Recognition of paleoearthquakes on the Puente Hills blind thrust fault, California, *Science*, *300*, 115–118.

Dragert, H., K. Wang, and T. S. James (2001), A silent slip event on the deeper Cascadia subduction interface, *Science*, *292*, 1525–1528.

Ekstrom, G., and P. England (1989), Seismic strain rates in regions of distributed continental deformation, *J. Geophys. Res.*, *94*, 10,231–10,257.

Field, E. H., D. D. Jackson, and J. F. Dolan (1999), A mutually consistent seismic-hazard source model for southern California, *Bull. Seismol. Soc. Am.*, *89*, 559–578.

Grant, L. B., and T. K. Rockwell (2002), A northward-propagating earthquake sequence in coastal southern California?, *Seismol. Res. Lett.*, *73*, 461–469.

Hanks, T. C., and H. Kanamori (1979), A moment magnitude scale, *J. Geophys. Res.*, *84*, 2348–2350.

Hauksson, E. (2000), Crustal structure and seismicity distribution adjacent to the Pacific and North America plate boundary in southern California, *J. Geophys. Res.*, *105*, 13,875–13,903.

Kagan, Y. Y. (2004), Southern California earthquakes: Extended sources, Univ. of Calif., Los Angeles. (available at http://scec.ess.ucla.edu/%7eykagan/relm_index.html)

Kostrov, B. V. (1974), Seismic moment and energy of earthquakes, and seismic flow of rock, *Izv. Acad. Sci. USSR Phys. Solid Earth*, *134*, 23–40.

Linde, A. T., M. T. Gladwin, M. J. S. Johnston, R. L. Gwyther, and R. G. Bilham (1996), A slow earthquake sequence on the San Andreas fault, *Nature*, *383*, 65–68.

McGuire, J. J., and P. Segall (2003), Imaging of aseismic fault slip transients recorded by dense geodetic networks, *Geophys. J. Int.*, *155*, 778–788.

Meade, B. J., and B. H. Hager (2005), Block models of crustal motion in southern California constrained by GPS measurements, *J. Geophys. Res.*, *110*, B03403, doi:10.1029/2004JB003209.

Meade, B. J., B. H. Hager, S. C. McClusky, R. E. Reilinger, S. Ergintav, O. Lenk, A. Barka, and H. Ozener (2002), Estimates of seismic potential in the Marmara Sea region from block models of secular deformation constrained by Global Positioning System measurements, *Bull. Seismol. Soc. Am.*, *92*, 208–215.

Okada, Y. (1985), Surface deformation due to shear and tensile faults in a half space, *Bull. Seismol. Soc. Am.*, *75*, 1135–1154.

Peltzer, G., F. Crampe, S. Hensley, and P. Rosen (2001), Transient strain accumulation and fault interaction in the Eastern California Shear Zone, *Geology*, *29*, 975–978.

Petersen, M. D., W. A. Bryant, C. H. Cramer, T. Cao, M. S. Reichle, A. D. Frankel, J. J. Lienkaemper, P. A. McCrory, and D. P. Schwartz (1996), Probabalistic seismic hazard assessment for the State of California, *U.S. Geol. Surv. Open File Rep., 96-706*. (available at http://www.consrv.ca.gov/CGS/rghm/psha/ofr9608/index.htm)

Rockwell, T. K., S. Lindvall, M. Herzberg, D. Murback, T. Dawson, and G. Berger (2000), Paleoseismology of the Johnson Valley, Kickapoo, and Homestead Valley faults: Clustering of earthquakes in the Eastern California Shear Zone, *Bull. Seismol. Soc. Am.*, *90*, 1200–1236.

Rubin, C. M., S. C. Lindvall, and T. K. Rockwell (1998), Evidence for large earthquakes in metropolitan Los Angeles, *Science*, *281*, 398–402.

Sauber, J., W. Thatcher, S. C. Solomon, and M. Lisowski (1994), Geodetic slip rate for the Eastern California Shear Zone and the recurrence time of Mojave Desert earthquakes, *Nature*, *367*, 264–266.

Savage, J. C., M. Lisowski, and W. H. Prescott (1990), An apparent shear zone trending north-northwest across the Mojave Desert into Owens Valley, eastern California, *Geophys. Res. Lett.*, *17*, 2113–2116.

Scholz, C. H. (1998), Earthquakes and friction laws, *Nature*, *391*, 37–42.

Shaw, J. H., and P. M. Shearer (1999), An elusive blind-thrust fault beneath metropolitan Los Angeles, *Science*, *283*, 1516–1518.

Shen-Tu, B., W. E. Holt, and A. J. Haines (1999), Deformation kinematics in the western United States determined from Quaternary fault slip rates and recent geodetic data, *J. Geophys. Res.*, *104*, 28,927–28,955.

Sieh, K. E. (1978), Slip along the San Andreas fault associated with the great 1857 earthquake, *Bull. Seismol. Soc. Am.*, *68*, 1421–1447.

Sieh, K. (1996), The repetition of large-earthquake ruptures, *Proc. Natl. Acad. Sci. U.S.A.*, *93*, 3764–3771.

Sieh, K. E., and P. L. Williams (1990), Behavior of the southernmost San Andreas fault during the past 300 years, *J. Geophys. Res.*, *95*, 6629–6645.

Sieh, K., M. Stuiver, and D. Brillinger (1989), A more precise chronology of earthquakes produced by the San Andreas fault in southern California, *J. Geophys. Res.*, *94*, 603–623.

Stein, R. S., and T. C. Hanks (1998), M $\geq$ 6 earthquakes in southern California during the twentieth century: No evidence for a seismicity or moment deficit, *Bull. Seismol. Soc. Am.*, *88*, 635–652.

Vincent, P. (2000), Aseismic slip events along the southern San Andreas fault system captured by radar interferometry, in Proceedings of the 3rd Conference on Tectonic Problems of the San Andreas Fault System, 16 pp., Stanford Univ., Stanford, Calif. (available at http://pangea.stanford.edu/GP/sanandreas2000)

Vincent, P., J. B. Rundle, R. Bilham, and S. M. Buckley (1998), Aseismic creep along the San Andreas and Superstition Hills faults with uplift at Durmid Hill, southernmost San Andreas fault, CA measured by radar interferometry, *Eos Trans. AGU*, *79*(45), Fall Meet. Suppl., F184.

Ward, S. N. (1998a), On the consistency of earthquake moment rates, geologic fault data, and space geodetic strain: The United States, *Geophys. J. Int.*, *134*, 172–186.

Ward, S. N. (1998b), A deficit vanished, *Nature*, *394*, 827–829.

Weldon, R. J., and K. E. Sieh (1985), Holocene rate of slip and tentative recurrence interval for large earthquakes on the San Andreas fault, Cajon Pass, southern California, *Geol. Soc. Am. Bull.*, *96*, 793–812.

Wells, D. L., and K. J. Coppersmith (1994), New empirical relationships among magnitude, rupture length, rupture width, rupture area, and surface displacement, *Bull. Seismol. Soc. Am.*, *84*, 974–1002.

Working Group on California Earthquake Probabilities (1995), Seismic hazards in southern California: Probable earthquakes, 1994 to 2024, *Bull. Seismol. Soc. Am.*, *85*, 379–439.

B. H. Hager, Department of Earth, Atmospheric and Planetary Sciences, Massachusetts Institute of Technology, Cambridge, MA 02139, USA.

B. J. Meade, Department of Earth and Planetary Sciences, Harvard University, 20 Oxford St., Cambridge, MA 02138, USA. (meade@rupture.harvard.edu)